ACTIVE AND PASSIVE MICROWAVE REMOTE SENSING OF SPRINGTIME NEAR-SURFACE SOIL THAW EVENTS AT MIDDLE LATITUDES

L. Han*[a], A. Tsunekawa [a], and M. Tsubo [a]

[a] Arid Land Research Center, Tottori University, 1390 Hamasaka, Tottori 680-0001, Japan
(han, tsunekawa, Tsubo)@alrc.tottori-u.ac.jp

Technical Commission VII Symposium 2010

KEY WORDS: Snow Ice; Soil; Application; Estimation; Algorithms; Radar; Passive

ABSTRACT:

Springtime near-surface soil thaw event is important for understanding the near-surface earth system. Previous researches based on both active and passive microwave remote sensing technologies have paid scant attention, especially at middle latitudes where the near-surface earth system has been changed substantially by climate change and human activities, and are characterized by more complex climate and land surface conditions than the permafrost areas. SSM/I brightness temperature and QuikSCAT Ku-band backscatter were applied in this study at a case study area of northern China and Mongolia in springtime of 2004. The soil freeze–thaw algorithm was employed for SSM/I data, and a random sampling technique was applied to determine the brightness temperature threshold for 37 GHz vertically polarized radiation: 258.2 and 260.1 K for the morning and evening satellite passes, respectively. A multi-step method was proposed for QuikSCAT Ku-band backscatter based on both field observed soil thaw events and the typical signature of radar backscatter time series when soil thaw event occurred. The method is mainly focuses on the estimated boundary of thaw events and detection of primary thaw date. The passive microwave remote sensing (SSM/I) based result had a good relationship with the near-surface soil temperature, while the active microwave remote sensing (QuikSCAT) based result had both relationships with temperature and soil moisture conditions. And also, QuikSCAT result identifies the geographical boundary of water-drove thaw event, which is crucial for understanding the different types of springtime near-surface soil thaw at middle latitudes.

1. INTRODUCTION

Near-surface soil freeze–thaw cycles have an important role in earth systems and directly affect the terrestrial hydrological cycle. Remote sensing provides an effective way for such event detection, especially, the microwave remote sensing (Zhang, et al., 2004). Microwave remote sensing based near-surface soil thaw event detection at mid-latitudes where near-surface changing seriously still rare (Han, et al., 2010). Generally, in active microwave remote sensing, the thaw event was detected based on the radar backscatter change which is responded to the dielectric constant of the surface; and in passive microwave remote sensing, the thaw event was detected based on the brightness temperature's increasing.

Scant attentions have paid in mid-latitude areas, which suggested our objectives as follows: 1) to detect and validate springtime soil thaw event by passive and active microwave remote sensing data; 2) to understand the difference in the results from active and passive microwave remote sensing data.

2. STUDY AREA

Our study area (Figure 1) lies between latitudes 31°N and 55°N and longitudes 71°E and 136°E including different humidity zones from arid to humid.

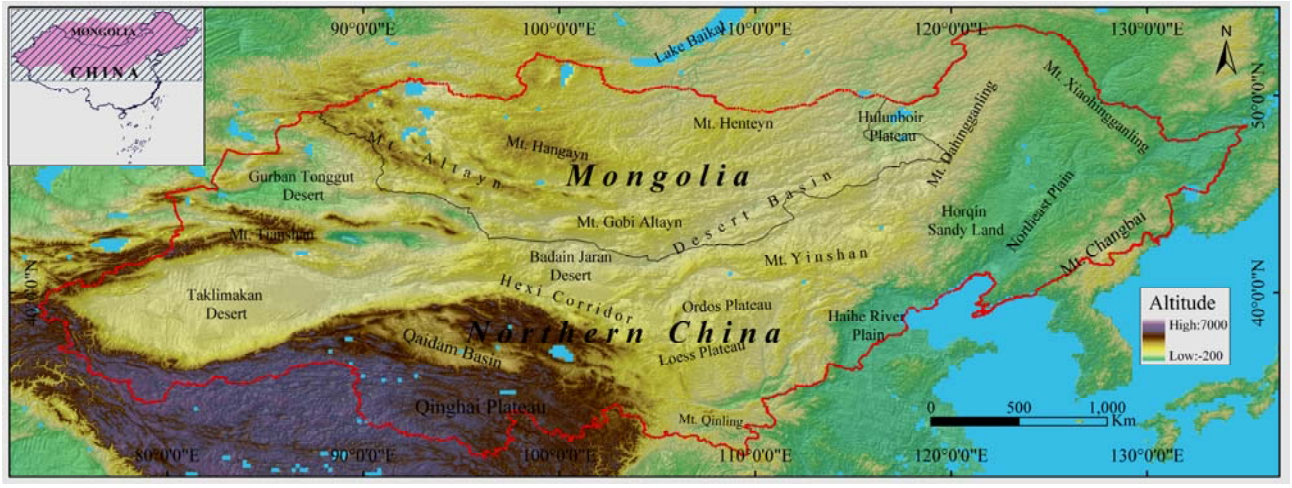

Figure 1. Study area

* Corresponding author

There are strong regional climatic differences within the area and a diverse range of vegetation and land surface including large areas of desert, desert steppe, steppe, forested steppe, and forest. The elevation also has large range from more than 4000m at high mountain areas and Tibetan Plateau to near 0 at the east beach. Vegetation degeneration and extreme environmental events (e.g. sandstorm) are also undergoing or frequently happened (Tsunekawa, et al., 2005; Zhang, et al., 2008). Its various conditions in middle latitude areas make the essential of understanding springtime soil thaw event in this area.

3. MATERIALS AND PREPROCESSING

3.1. Microwave remote sensing records

A practical active microwave remote sensing data, QuikSCAT Ku-band measurement, was acquired from NASA's Jet Propulsion Laboratory as their level 2A product. First, all backscatter measurements at the first 180 days of 2004 were extracted and averaged on a daily basis; second, a grid format time series with 25×25 km spatial resolution was produced by spatially interpolating from the averaged backscatter daily times series. And the out-beam record was adopted in this work because of its wider swath.

Brightness temperature data from Special Sensor Microwave/Imager (SSM/I), provided by National Snow and Ice Data Center, was adopted in this work, as the passive microwave remote sensing data. We used the 19 and 37 GHz vertically polarized brightness temperature ($T_{B.19V}$ and $T_{B.37V}$) data from both ascending and descending tracks at the first 180 days of 2004. This data also have a spatial resolution of 25×25 km. Because daily SSM/I data did not cover the whole study area, we used time series of brightness temperature by 7-day maximum/minimum combined with considering about the revisit period of SSM/I in our study area.

3.2. Soil temperature and moisture data

We obtained soil temperatures and moisture recorded at five reference sites used in the Coordinated Energy and Water Cycle Observation Project from the Centralized Integrated Data Archive (http://www.ceop.net/) and selected three of the five stations on the basis of their location and the period covered by their data. Soil temperatures and moistures recorded at Shenmu in northern China and Bayan-Unjuul in Mongolia were also included in our study. We used soil temperatures measured at 5 cm depth because most microwave radiation emitted at the surface emerges from the top layer of soil (Zwally and Gloersen, 1977).

3.3. Meteorological records

The Global Summary of the Day product from the National Climate Data Center of United States was applied in our study. Daily air temperature, precipitation, and snow depth observations were used to support interpretation of springtime thaw events from the QuikSCAT backscatter time series and to estimate the soil moisture by using a water balance based model.

4. METHODOLOGY

4.1. Active microwave remote sensing method

The method in this work is based on our previous approach (Han, et al., 2010b), which studied the typical backscatter signatures when springtime soil thaw occurred and suggested the method for the thaw event deriving from QuikSCAT time series.

Geographical boundary is firstly detected by Equation 1.

$$Slope = \frac{n \times \sum_{i=1}^{n} i \times \delta_i - \left(\sum_{i=1}^{n} i\right)\left(\sum_{i=1}^{n} \delta_i\right)}{n \times \sum_{i=1}^{n} i^2 - \left(\sum_{i=1}^{n} i\right)^2} \quad (1)$$

Where $Slope$ is the trend of QuikSCAT backscatter with the unit dB serving as the indicator for boundary clarification; n represents analyzed range in every 5-day step; i is the each 5-day period, $i=1$ for the 5-day period from the 1st day of year (DOY) to the 5th DOY, $i=2$ for the 5-day period from the 6th DOY to the 10th DOY, …; and δ_i is the average QuikSCAT backscatter of the each 5-day i. $Slope$ larger than 0 identifies an area of no thaw event, and $Slope$ less than 0 identifies an area in which a thaw event occurred.

a primary thaw date, which defines as the middle day of a short period in which backscatter data are most diverse which is deduced as the most significant soil dielectric constant change driving by dominated amount soil water's state changing from ice to liquid water, is estimated by equations as shown below.

$$PI(i) = Stdev(sigma0_{i-n} : sigma0_{i+n}) \quad (2)$$

$$Ptd = i, when PI(i) = \max(PI(i)) \quad (3)$$

Where $PI(i)$ represents the primary thaw indicator on day i, which is a short period's standard deviation of QuikSCAT backscatter ($sigma0$) n days ($n=4$ was set in this research, plus the current day it also means 5-day's step) before and after day i; Ptd represents the primary thaw date when $PI(i)$ reaches its maximum. The primary thaw date is only calculated in the areas where soil thaw events happened as estimated in Equation 1.

4.2. Passive microwave remote sensing method

The soil freeze–thaw algorithm was adopted in this research, which requires two parameters: a negative spectral gradient between $T_{B.19V}$ and $T_{B.37V}$, as described by equation (4), and a threshold $T_{B.37V}$ as described by equation (5):

$$\frac{\partial T_B}{\partial f} \le 0 \quad (4)$$

$$T_{B.37V} \le T_{37}, \quad (5)$$

Where T_{37} is the threshold derived from the linear relationship between $T_{B,37V}$ and near-surface soil temperature. It is set as 258.2 K and 260.1 K for morning and evening satellite passes based on our previous results (Han, et al., 2010a).

And the pixels from water-covered areas and regions of high elevation (>3000m) were filtered by considering their influences on brightness temperature.

4.3. Soil moisture model

A simplified water balance based model, as shown in Equation 6, is used in this investigation (Yamaguchi and Shinoda, 2002). The top 30 mm soil moisture content at the end of 2003 and the snow water equivalent after consecutive maximum temperature higher than 0°C at the beginning of 2004 were considered in estimating the soil moisture conditions.

$$dW(t)/dt = P(t) - E(t) - R(t)$$
$$and \qquad (6)$$
$$R(t) = \begin{cases} W(t) - W_{fc}, & W(t) > W_{fc} \\ 0, & W(t) \le W_{fc} \end{cases}$$

Where W, the soil moisture, is expressed as the equivalent depth of liquid water that exists from the surface to a 30-cm depth, and t is the time in days; P, E, R represent the precipitation, evapotranspiration and runoff, respectively; and W_{fc} represents the field capacity.

5. RESULTS AND DISCUSSION

5.1. Validations of the results

Validations have done for both of the results from active and passive microwave remote sensing. For result from active microwave remote sensing, a reliability of R = 0.8, P < 0.05 was obtained between estimated primary thaw date and the date when consecutive days' average air temperature keeping positive values; and R = 0.85, P < 0.05 was obtained in result from passive microwave remote sensing with comparison between estimated onset/offset of the thaw and field measured soil thaw event. And the soil moisture model was validated by comparison with the ground truth with root mean square error (RMSE) of 4.10±1.69 mm. Such reliabilities were strongly enhanced our confidence in making the further analysis.

5.2. Result from active microwave remote sensing

Primary thaw date and geographical boundary of the thaw was detected as shown in Figure 2. In the north: the thaw event boundary runs south of the Three River Plain, Mt. Xiaohingganling, and Mt. Dahingganling to the north of the Desert Basin, then to the south of Mt. Henteyn, Mt. Hangayn, and Mt. Altayn. The other area consists of regions of high elevation, such as Mt. Tianshan, Mt. Changbai, and the Tibetan Plateau. No thaw events occurred in the remaining (gray) areas, like the deserts regions and south warmer areas, due to the drier surface conditions or temperatures too high to freeze the surface layer in winter. The primary thaw date follows clear spatial and temporal patterns. In high elevation and high northern areas, thaw events happen later than in lower elevation and southern areas. On the Tibetan Plateau, at Mt. Hangayn, and at Mt. Altayn, the thaw event occurred at the end of the first 180 days. Those three areas are almost entirely covered by permafrost, so only the active layer thaws in the short summer.

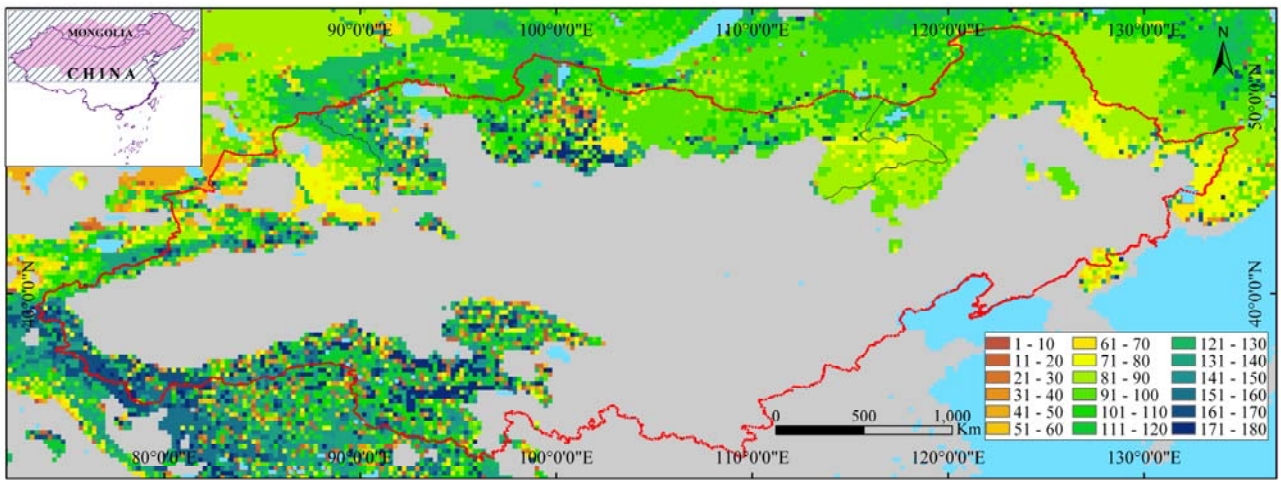

Figure 2. Primary thaw date and geographical boundary of the thaw derived from QuikSCAT data (Julian day). (Gray-colored areas represent regions without water driven soil thaw occurrence.)

5.3. Result from passive microwave remote sensing

Onset and offset of springtime soil thaw event was obtained as shown in figure 3. The onset and offset of near-surface soil thawed in spring begins in the south and southeast of the study area and then progresses northwest and north, but these trends are somewhat disrupted in areas of complex topography.

The main progression of the onset is from Mt. Qinling through the Guanzhong Basin, Loess Plateau, Ordos Plateau, and on toward Mt. Yinshan, the Mongolian Plateau, and finally to the Desert Basin and Hulunboir Plateau. This progression is disrupted by high elevations at Mt. Yinshan and Mt. Henteyn. Another extension of the onset branches northwest from the main northern trend at the Loess Plateau, and extends approximately northwest through the Hexi Corridor and Badain Jaran Desert to Mt. Altayn, where the latest onset of near-surface soil thawed is evident. The third branch of the onset progresses approximately northeast through Haihe River Plain to the Horqin Sandy Land, Northeast Plain, and Songnen Plain,

and then to Mt. Dahingganling, Mt. Xiaohingganling and Three River Plain (also known as the Sanjiang Plain). This progression is disrupted by the high elevation of Mt. Changbai. The onset of near-surface soil frozen begins early in the Gurban Tonggut and Taklimakan deserts, which can perhaps be attributed to these areas being at lower elevations than surrounding areas and having less soil water.

The earliest offset of near-surface soil frozen occurs at Mt. Qinling. It then progresses to the northwest through the Guanzhong Basin, along the west of the Loess Plateau, through the Hexi Corridor and Badain Jaran Desert, and finally to Mt. Altayn and Mt. Hangayn. To the east of the Badain Jaran Desert and Hexi Corridor, the offset of near-surface soil frozen arrives earlier than in surrounding regions. From Mt. Qinling, the offset progresses north to the Guanzhong Basin, and continues along the area south of Mt. Luliang and Mt. Taihang, then to the Loess and Ordos plateaus and through to Mt. Yinshan, the Mongolian Plateau, and the Desert Basin, until the latest offset of near-surface soil frozen occurs on the Hulunboir Plateau and at Mt. Henteyn. The offset of near-surface soil frozen also progresses northeast from the Haihe River Plain along the coast to the Horqin Sandy Land, and then to the surrounding areas of Mt. Dahingganling, Mt. Xiaohingganling, the Northeast Plain, Mt. Changbai, with the latest offset of near-surface soil frozen occurring to the north of Mt. Dahingganling and the Three River Plain.

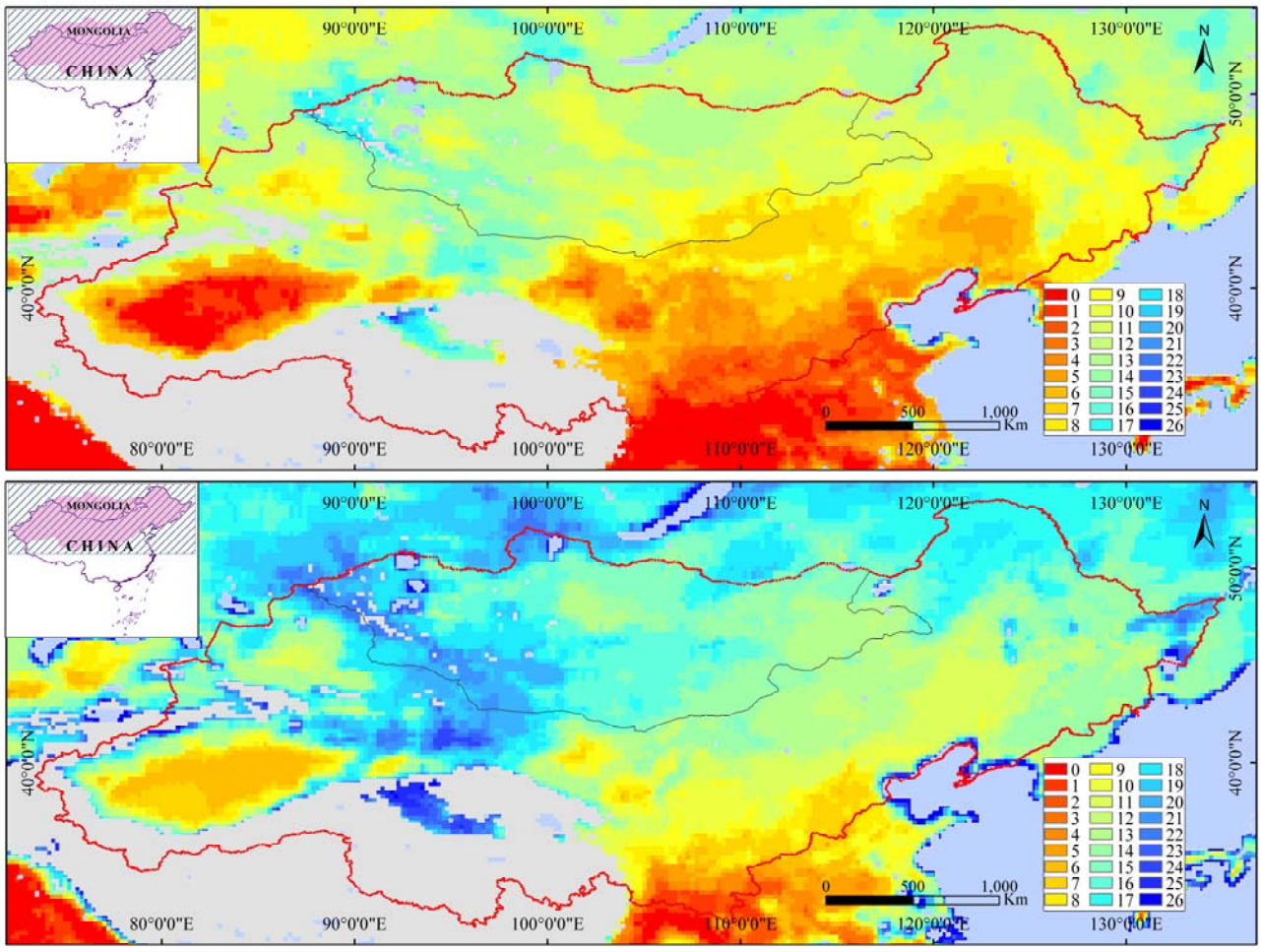

Figure 3. Onset (upper) and offset (nether) of springtime soil thaw derived from SSM/I brightness temperature (Julian week). (Gray-colored areas are the high elevation regions)

5.4. Difference in the results

Result that derived from SSM/I brightness temperature was almost relied on the T_{37} which have significant linear relationship with near-surface soil temperature. From which, we can deduce that the results derived from SSM/I brightness temperature is sensitive to near-surface soil temperature, which is why soil thaw event could be detected in desert regions.

Result that derived from QuikSCAT backscatter time series has regions both soil thaw event occurrence and no soil thaw event occurrence. From the analysis of average air temperature and modeled soil moisture as shown in figure 4, the difference between samples with/without soil thaw event happened could be clarified: 1) samples with thaw event detected by QuikSCAT backscatter had an average air temperature of -15.29±4.29 °C with soil moisture of 38.27±21.96 mm in the month of thaw event happened; and 2) samples without thaw event detected by QuikSCAT backscatter had an average air temperature of -1.80±6.37 °C with soil moisture of 35.77±24.63 mm in the month when air temperature switch from negative values to positive values. And at the areas where air temperature keeping negative for a long period but no thaw event detected could easily deduce that the region has no enough soil water content to freeze.

The difference of the results derived from active and passive microwave remote sensing time series is essential for understanding the near-surface earth system changes. The SSM/I's result could indicate the soil temperature switch from negative to positive values, while the QuikSCAT's result could deduce the soil water states change from ice to liquid water. Such kind of phenomenon would be related to the climate change and extreme environment (e.g. springtime dust emission) in this area for better understanding the Earth surface interactions.

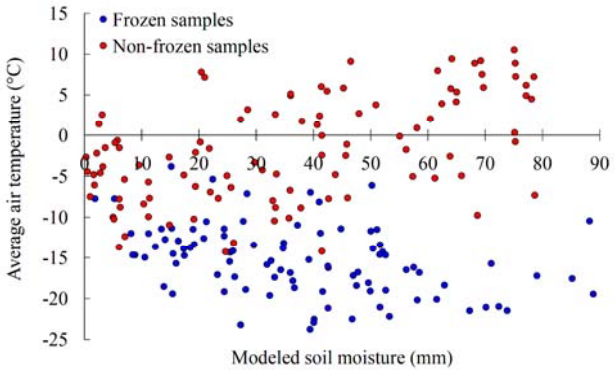

Figure 4. Near-surface air temperature and soil moisture conditions' difference between samples with/without soil thaw events detected by QuikSCAT backscatter.

6. CONCLUSION

SSM/I brightness temperature and QuikSCAT Ku-band backscatter were applied in this study at a case study area of northern China and Mongolia in springtime of 2004. Conclusions could be approached as follows:

1) Both soil freeze-thaw algorithm for SSM/I brightness temperature and multi-step method for QuikSCAT backscatter were effective for springtime near-surface soil thaw events detection. A reliability of $R = 0.8$, $P < 0.05$ was obtained between estimated primary thaw date and the date when consecutive days' average air temperature keeping positive values; and $R = 0.85$, $P < 0.05$ was obtained in result from passive microwave remote sensing with comparison between estimated onset/offset of the thaw and field measured soil thaw event.

2) The passive microwave remote sensing (SSM/I) based result had a good relationship with the near-surface soil temperature, while the active microwave remote sensing (QuikSCAT) based result had both relationships with temperature and soil moisture conditions, especially soil moisture conditions. And also, QuikSCAT result identifies the geographical boundary conditions of the thaw event in springtime of 2004, which is crucial for understanding the different types of springtime near-surface soil thaw at middle latitudes.

Since both SSM/I brightness temperature and QuikSCAT backscatter are available from 1999 to 2009, further analysis is undergoing for understanding the interaction of springtime soil thaw event with other near-surface events.

REFERENCES

Han, L., Tsunekawa, A., Tsubo, M., 2010a. Monitoring near-surface soil freeze–thaw cycles in northern China and Mongolia from 1998 to 2007. *International Journal of Earth Observation and Geoinformation*, doi: 10.1016/j.jag.2010.04.009.(in press)

Han, L., Tsunekawa, A., Tsubo, M., 2010b. Radar remote sensing of springtime near-surface soil thaw events at mid-latitudes. Submitted to *International Journal of Remote Sensing.*

Tsunekawa, A., Ito, T. Y., Shinoda, M., Nemoto, M., Suhama, T., Ju, H., Shimizu, H. 2005. Methodology for assessment of desertification based on vegetation degradation using net primary productivity (NPP) as a key indicator. *Phyton*, 45, 185–192.

Yamaguchi, Y. and Shinoda, M. (2002). Soil moisture modeling based on multiyear observations in the Sahel. Journal of Applied Meteorology, 41, 1140–1146.

Zhang, B., Tsunekawa, A., Tsubo, M. 2008. Contributions of sandy lands and stony deserts to long-distance dust emission in China and Mongolia during 2000–2006. *Global and Planetary Change*, 60, 487–504.

Zhang, T., Barry, R. G., Armstrong, R. L., 2004. Application of satellite remote sensing techniques to frozen ground studies. *Polar Geography*, 28, 163–196.

Zwally, H. J., and Gloersen, P., 1977. Passive microwave images of the Polar Regions and research applications. *Polar Record*, 18, 431–450.